Photosynthesis

DOI: 10.1002/anie.201404664

Photocatalytic Water Oxidation by a Mixed-Valent $Mn^{III}_3Mn^{IV}O_3$ Manganese Oxo Core that Mimics the Natural Oxygen-Evolving Center**

Rami Al-Oweini, Andrea Sartorel, Bassem S. Bassil, Mirco Natali, Serena Berardi, Franco Scandola, Ulrich Kortz,* and Marcella Bonchio**

Abstract: *The functional core of oxygenic photosynthesis is in charge of catalytic water oxidation by a multi-redox Mn^{III}/Mn^{IV} manifold that evolves through five electronic states (S_i, where $i = 0$–4). The synthetic model system of this catalytic cycle and of its $S_0 \rightarrow S_4$ intermediates is the expected turning point for artificial photosynthesis. The tetramanganese-substituted tungstosilicate $[Mn^{III}_3Mn^{IV}O_3(CH_3COO)_3(A\text{-}\alpha\text{-}SiW_9O_{34})]^{6-}$ (Mn_4POM) offers an unprecedented mimicry of the natural system in its reduced S_0 state; it features a hybrid organic–inorganic coordination sphere and is anchored on a polyoxotungstate. Evidence for its photosynthetic properties when combined with $[Ru(bpy)_3]^{2+}$ and $S_2O_8^{2-}$ is obtained by nanosecond laser flash photolysis; its $S_0 \rightarrow S_1$ transition within milliseconds and multiple-hole-accumulating properties were studied. Photocatalytic oxygen evolution is achieved in a buffered medium (pH 5) with a quantum efficiency of 1.7 %.*

The oxygen-evolving complex of photosystem II (PSII-OEC) in green plants, algae, and cyanobacteria is the unique catalytic site where, upon illumination, H_2O is oxidized to form O_2.[1] The natural OEC is a tetramanganese calcium oxo cluster (Mn_4O_5Ca) that is harbored within the PSII complex, with a flexible and adaptive coordination environment provided by the protein residues.[2] In particular, carboxylate ligands play a major role in the assembly of the OEC cluster by bridging Mn ions and the Ca^{2+} site. Dynamic binding throughout a sequence of five one-electron-step redox states (S_i, where $i = 0$–4) underpins the efficient photo-induced water oxidation that is catalyzed by the PSII-OEC and occurs under visible-light irradiation and with an exceptional turnover frequency (TOF) of 100–400 s^{-1}.[3] The Achilles' heel of the PSII-OEC lies in its conceivable fragility and its mutable asset, which hampers a precise mapping of the geometry and electronic configuration for all $S_0 \rightarrow S_4$ intermediates (Figure 1). Indeed, the available X-ray data refer to an ill-defined average of highly reduced cluster states (S_{-i}), which are likely formed under beam irradiation, but not directly involved in the photosynthetic cycle. A structural

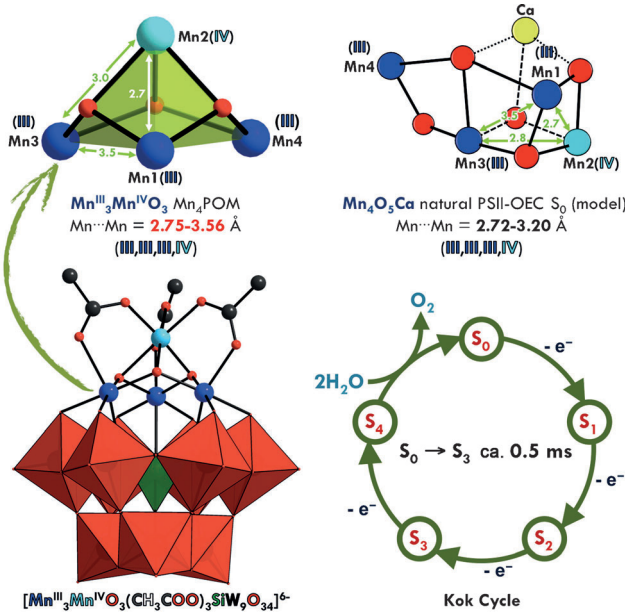

Figure 1. Combined polyhedral/ball-and-stick representation of Mn_4POM (bottom left, counter cations and water molecules in the crystal are not shown for clarity). Comparison of the Mn_4POM core (top left) with the S_0 state of the natural OEC as described by a quantum mechanics/molecular mechanics (QM/MM) model (top right).[4] Photo-induced electron flow within the $S_0 \rightarrow S_4$ Kok cycle of the natural PSII-OEC (bottom right). Balls: calcium yellow, carbon dark grey, manganese(III) blue, manganese(IV) light blue, oxygen red; polyhedra: SiO_4 green, WO_6 red.

[*] Dr. R. Al-Oweini, Dr. A. Sartorel, Dr. S. Berardi, Prof. M. Bonchio
ITM-CNR and Dipartimento di Scienze Chimiche, Università di Padova
via Marzolo 1, 35131 Padova (Italy)
E-mail: marcella.bonchio@unipd.it
Homepage: http://www.chimica.unipd.it/NanoMolCat
Dr. B. S. Bassil, Prof. U. Kortz
Jacobs University, School of Engineering and Science
P.O. Box 750561, 28725 Bremen (Germany)
E-mail: u.kortz@jacobs-university.de
Homepage: http://www.jacobs-university.de/ses/ukortz
Dr. M. Natali, Prof. F. Scandola
Dipartimento di Scienze Chimiche e Farmaceutiche, Università di Ferrara and Centro Interuniversitario per la Conversione Chimica dell'Energia Solare, sez. di Ferrara
via Fossato di Mortara 17–19, 44121 Ferrara (Italy)
E-mail: snf@unife.it

[**] This work was supported by the Italian MIUR (FIRB "NanoSolar" RBAP11C58Y, PRIN "Hi-Phuture" 2010N3T9M4_001) and by the Fondazione Cariparo (Nanomode, progetti di eccellenza 2010). The EU COST Action program (CM1003, CM1203, and CM1205) is gratefully acknowledged. U.K. thanks the German Science Foundation (DFG, KO-2288/20-1) and Jacobs University for research support. Figure 1 was generated with Diamond Version 3.2 (copyright Crystal Impact GbR).

Supporting information for this article is available on the WWW under http://dx.doi.org/10.1002/anie.201404664.

model for the S_0 initial state is only available in silico, addressing the starting point of the OEC four-electron oxidative staircase.[4] In agreement with EXAFS and EPR results, the computational model for the OEC S_0 state shows a mixed-valent Mn_4(III,III,III,IV) core with two short Mn···Mn distances (ca. 2.7 Å) and two longer ones (up to 3.2 Å).[4]

To mimic structure and activity of the PSII-OEC, special attention has been dedicated to tetranuclear metal catalysts, including Mn-based complexes.[5] However, only few ruthenium or cobalt tetrametallic cores have been recognized as feasible oxygen-evolving catalysts under photocatalytic conditions.[5] We focus herein on a unique tetramanganese core that is stabilized by a hybrid set of ligands, including an all-inorganic tungstosilicate platform and three acetate bridges. The resulting polyanion, $[Mn^{III}_3Mn^{IV}O_3(CH_3COO)_3(A\text{-}\alpha\text{-}SiW_9O_{34})]^{6-}$ (Mn_4POM), displays striking similarities with the natural OEC in its S_0 state compared to the Mn_4 oxo structure and its Mn^{III}/Mn^{IV} mixed valency (Figure 1). Our results confirm that Mn_4POM undergoes fast and multiple electron transfers under visible-light irradiation, leading to water photooxidation and oxygen evolution. The structural analogy with the natural photosynthetic catalyst is thus nicely complemented by a unique functional behavior, which follows a bio-inspired mechanism (Figure 1).

Mn_4POM is readily synthesized in aqueous solution (sodium acetate buffer, pH 6) and on a gram scale by reaction of the mixed-valence compound $[Mn^{III}_8Mn^{IV}_4O_{12}(CH_3COO)_{16}(H_2O)_4]\cdot 2\,CH_3COOH\cdot 4\,H_2O$ (Mn_{12}) with $Na_{10}[A\text{-}\alpha\text{-}SiW_9O_{34}]$ in a 1:1 molar ratio at room temperature.[6] The key motif is a $Mn^{III}_3Mn^{IV}O_3$ core with a defective cubane arrangement, which differs from that of literature analogues (Figure 1).[7,8] Three μ-acetate bridges define the geometry of the $Mn^{III}_3Mn^{IV}O_3$ core, with $Mn^{III}\cdots Mn^{IV}$ distances in the range of 2.749(6)–2.955(6) Å.[6] These structural features show a direct correspondence with the calculated geometry of the natural PSII-OEC S_0 state, where $Mn^{III}\cdots Mn^{IV}$ distances fall in the range of 2.7–3.2 Å (Figure 1; see also the Supporting Information, Table S1).[4]

According to the bio-inspired Kok cycle and the envisaged $S_0\rightarrow S_4$ four-electron transfer mechanism (Figure 1), one key requirement for efficient electrocatalytic water oxidation is a sequential multi-electron oxidation in a narrow potential window. Therefore, we have addressed the oxidation manifold of the synthetic Mn_4POM to go beyond the S_0 state analogy.

In the oxidative scan, cyclic voltammetry (CV) of Mn_4POM [0.5 mM in $Na_2SiF_6/NaHCO_3$ buffer (50 mM), Na_2SO_4 (0.5 M), pH 5.2] shows one broad anodic wave at a peak potential of $E_a = 0.87$ V versus Ag/AgCl, which stems from a multi-electron oxidation of the Mn core (three electrons according to Cottrell equation analysis, in agreement with literature evidence; Figure S1).[6] This process is then followed by the onset of a strong catalytic wave that is due to water oxidation, ($E = 1.25$ V vs. Ag/AgCl, overpotential = 0.53 V; Figure S1).[9]

For applications within artificial photosynthesis, the final aim is to power the Mn_4POM $S_0\rightarrow S_4$ manifold by light irradiation. This is expected to occur through multiple photo-induced electron transfers, with concomitant generation of high-valent Mn-based reactive states, enabling the water oxidation cycle and oxygen evolution. Therefore, we have explored the photocatalytic potential of Mn_4POM in a so-called sacrificial system with $[Ru(bpy)_3]^{2+}$ (bpy = 2,2′-bipyridine) as the visible-light photosensitizer and sodium persulfate ($Na_2S_2O_8$) as a terminal electron acceptor.[5] In such a system, the $[Ru(bpy)_3]^{3+}$ oxidant is photo-generated by oxidative quenching of the $*[Ru(bpy)_3]^{2+}$ excited state with persulfate and by a second dark reaction that involves the sulfate radical $SO_4^{-\bullet}$ [Eq. (1)–(3) in Figure 2].[10,11] Under the

$$[Ru(bpy)_3]^{2+} + h\nu \rightarrow *[Ru(bpy)_3]^{2+} \quad (1)$$
$$*[Ru(bpy)_3]^{2+} + S_2O_8^{2-} \rightarrow [Ru(bpy)_3]^{3+} + SO_4^{2-} + SO_4^{-} \quad (2)$$
$$[Ru(bpy)_3]^{2+} + SO_4^{-} \rightarrow [Ru(bpy)_3]^{3+} + SO_4^{2-} \quad (3)$$
$$3\,[Ru(bpy)_3]^{3+} + Mn_4POM \rightarrow 3\,[Ru(bpy)_3]^{2+} + Mn_4POM\,[3\,h^+] \quad (4)$$
$$Mn_4POM\,[3\,h^+] + SO_4^{-} + 2\,H_2O \rightarrow Mn_4POM + SO_4^{2-} + O_2 + 4\,H^+ \quad (5)$$

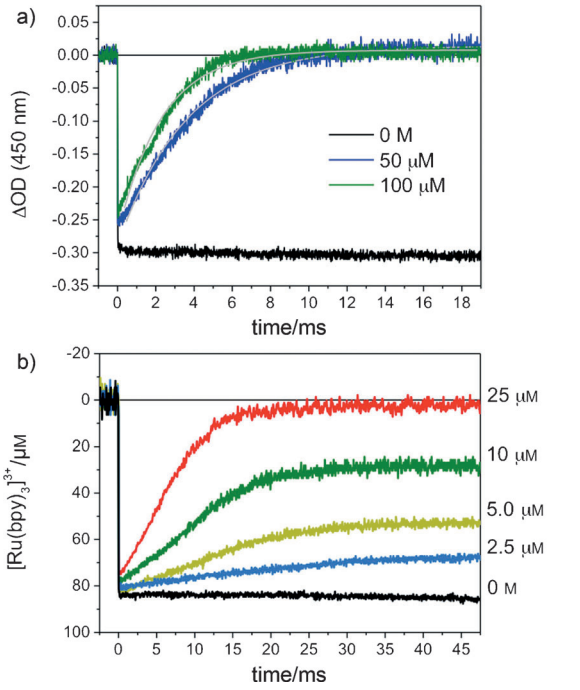

Figure 2. Laser flash photolysis experiments ($\lambda_{exc} = 355$ nm) in $NaHCO_3/Na_2SiF_6$ buffer (50 mM, pH 5.2) containing a) $[Ru(bpy)_3]^{2+}$ (50 μM), Mn_4POM (0–100 μM), and $S_2O_8^{2-}$ (5 mM; with related mono-exponential fitting), or b) $[Ru(bpy)_3]^{2+}$ (100 μM), Mn_4POM (0–25 μM), and $S_2O_8^{2-}$ (5 mM).

conditions explored, photo-generated $[Ru(bpy)_3]^{3+}$ ($E =$ 1.06 V vs. Ag/AgCl) is expected to leverage the three-electron ($S_0\rightarrow S_3$) oxidation of Mn_4POM [Eq. (4) in Figure 2], whereas the SO_4^{-} radical ($E = 2.40$ V vs. Ag/AgCl) is likely to be responsible for the generation of higher-valent states and oxygen evolution [Eq. (5) in Figure 2].[12]

In this study, the photocatalytic cycle involving Mn_4POM was dissected and analyzed within two different time frames to address: 1) electron transfer (ET) kinetics spanning a millisecond time domain by laser flash photolysis and 2) oxygen-evolution kinetics, which were monitored over several tens of minutes. Fast ET between the photo-activated reaction center (RC) and the OEC is one prerogative of the natural PSII system, where the $S_0\rightarrow S_4$ Kok cycle takes place in a few

milliseconds. In this artificial cycle, ET from the Mn_4POM S_0 state to $[Ru^{III}(bpy)_3]^{3+}$ proceeds through a bimolecular process [Eq. (4) in Figure 2], and its rate is expected to have a major impact on the sensitizer stability and on the overall photocatalytic performance.[13] In the present system, the ET kinetics are conveniently probed by nanosecond laser flash photolysis upon the photo-generation of a suitable amount of $[Ru^{III}(bpy)_3]^{3+}$ [Eq. (1)–(3) in Figure 2], which is detected as an instantaneous bleach of the $[Ru^{II}(bpy)_3]^{2+}$ absorption ($\lambda = 450$ nm; negative ΔOD in Figure 2; ΔOD = differential optical density). ET from Mn_4POM is then expected to yield a "bleach recovery" (decay to the baseline in Figure 2), that is, the recovery of the $[Ru^{II}(bpy)_3]^{2+}$ metal-to-ligand charge transfer band ($\lambda = 450$ nm).[5] The latter observation is indicative of a parallel oxidation of the Mn_4POM S_0 state to a high-valent state.

Through proper experimental design, two pieces of information can thus be obtained from laser flash photolysis studies: 1) the second-order kinetic constant of the primary ET event from the catalyst to the photo-generated oxidant (Figure 2a), and 2) the number of electrons that can be extracted from Mn_4POM with excess $[Ru^{III}(bpy)_3]^{3+}$ within milliseconds (Figure 2b). In particular, laser flash photolysis performed under pseudo-first-order conditions ($[Mn_4POM] \gg [Ru(bpy)_3]^{3+}$) yielded quantitative recovery kinetics that obey a mono-exponential law (Figure 2a) with rates that are linearly dependent on the Mn_4POM concentration (Figure S4). A second-order rate constant, $k = (4.6 \pm 0.6) \times 10^6\ M^{-1}\ s^{-1}$, can thus be obtained for the primary ET event in the cycle, which corresponds to the Mn_4POM $S_0 \rightarrow S_1$ transition by photo-generated $[Ru(bpy)_3]^{3+}$. This value is significantly lower than literature benchmarks for Mn^{II} coordination complexes[14a] or other tetramanganese POM-based systems,[14b] and may be ascribed to the $Mn^{III} \rightarrow Mn^{IV}$ transition.[14] Significantly, no variations of the ET kinetics were observed by laser flash photolysis upon aging of the catalyst stock solution.[15,16]

The potential of Mn_4POM as a light-driven "hole accumulator" was assessed with laser flash photolysis using sub-stoichiometric amounts of Mn_4POM (0–25 μM) with respect to photo-generated $[Ru(bpy)_3]^{3+}$ (ca. 80 μM; Figure 2b), while extending the bleaching recovery analysis to a time scale of 50 ms (Figure 2b). On this time scale, the kinetic data confirm a well-behaved first-order dependence of the ET rate on the Mn_4POM concentration (Figure S6). Moreover, the absorption recovery reaches a plateau value that is consistent with a multi-electron oxidation of the catalyst core, and amounts to an average of three ET events, with concomitant reduction of three equivalents of $[Ru(bpy)_3]^{3+}$ per catalyst. These results highlight the evolution of the Mn core within a $S_0 \rightarrow S_3$ manifold by sequential electron extraction and preceding water oxidation, which supports the mechanistic scenario in Figure 2 [Eq. (4)].[17]

Oxygen evolution was observed in the presence of Mn_4POM (6.3–50 μM), $[Ru(bpy)_3]^{2+}$ (1 mM), and $S_2O_8^{2-}$ (5 mM) in $NaHCO_3/Na_2SiF_6$ buffer (50 mM, pH 5.2) under illumination with a 150 W tungsten lamp with a 375 nm cut-off filter (illumination spot of 1 cm diameter, with a power density of 90 mW cm^{-2}). Oxygen formation was immediately observed, leveling off to a plateau yield after 30–70 minutes of irradiation (Figure 3). Both the initial reaction rate and overall O_2 production depend on the catalyst concentration, with chemical yields in the range of 1.2–3.7% depending on the persulfate conversion, and a total turnover number for Mn_4POM of up to 5.2 (Table S2). The low chemical yield can be ascribed to the irreversible bleaching of the $[Ru(bpy)_3]^{2+}$ sensitizer, which occurs upon continuous irradiation and was confirmed by UV/Vis analysis of the used reaction mixture (Figure S8).[5] The competitive degradation of $[Ru(bpy)_3]^{2+}$ appears to be dominant especially at low catalyst loading (Figure S8), where the bimolecular scavenging of the reactive Ru^{III} state is slowed down. Indeed, the O_2 plateau yield increased when the Mn_4POM concentration was increased to up to 50 μM (Figure 3).

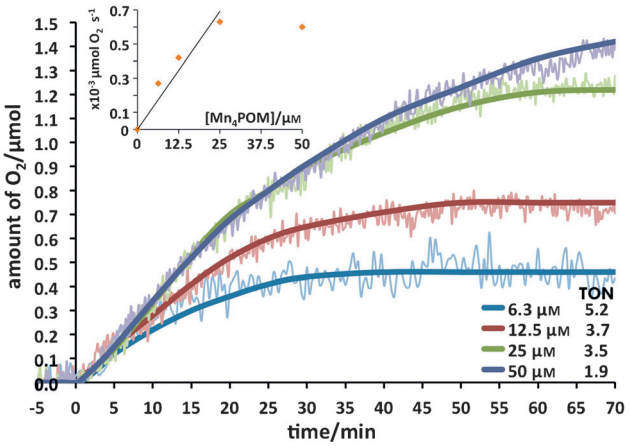

Figure 3. Oxygen production upon illumination of a solution containing Mn_4POM (6.3–50 μM), $[Ru(bpy)_3]^{2+}$ (1 mM), and $Na_2S_2O_8$ (5 mM) in $NaHCO_3/Na_2SiF_6$ buffer (50 mM; pH 5.2). Raw data are presented as light traces; smooth, dark lines were added for reasons of clarity. Inset: plot of the initial rate of O_2 production versus the Mn_4POM concentration.

Linear fitting of the reaction kinetics that were obtained 5–20 minutes after irradiation provided the initial rate of O_2 evolution (R_0, [μmol O_2 s^{-1}]), which also showed a well behaved first-order dependence on the Mn_4POM concentration below 25 μM and then levels off at higher catalyst concentrations (Figure 3; see also Figure S9 and Table S2). Turnover frequency (TOF) values per manganese center of up to $0.71 \times 10^{-3}\ s^{-1}$ were calculated: these values are significantly higher than those generally observed for bulk Mn oxides, which are on the order of $10^{-5}\ s^{-1}$ (Tables S2 and S3).[18,19]

Control experiments using an equimolar amount of Mn^{2+} ions, which were introduced as $MnSO_4 \cdot H_2O$, led to negligible O_2 production (Table S2). Moreover, the FT-IR features of the solid material that was recovered after the reaction are reminiscent of the fingerprint of pristine Mn_4POM (Figure S10). Altogether, these results are indicative of a mechanism for oxygen evolution that involves the four Mn centers of the catalyst core. A quantum efficiency[5] of 1.7% was calculated for a kinetic trace at a Mn_4POM concentration of 25 μM, when the reaction mixture was irradiated with

a monochromatic light-emitting diode (LED) emitting at 450 nm (power: 7 mW, photon flux: 2.63×10^{-8} einstein s^{-1}).

In conclusion, a novel strategy to access a synthetic Mn_4 oxygen-evolving center is based on the combined presence of an inorganic POM platform and carboxylate bridges. This hybrid set of ligands is used to shape a defective Mn_4 core with mixed valence, multi-redox properties, and photocatalytic behavior. The interplay of organic and inorganic residues provides a coordination environment with both stability and flexibility to assist stepwise one-electron oxidation of the catalytic core and to access high-valent Mn states that are responsible for water oxidation. Mn_4POM is the first manganese-containing POM that is catalytically active towards photo-induced water oxidation.[19] XAS spectroscopy will be used in the future to study the Mn-based manifold. Further work will be dedicated to tune the composite ligand set to lower the overpotential and increase quantum efficiency with the perspective of developing a regenerative photoelectrochemical cell.

Received: April 24, 2014
Revised: June 12, 2014
Published online: July 27, 2014

Keywords: flash photolysis · manganese · oxygen evolution · polyoxometalates · water oxidation

[1] J. Yano, V. Yachandra, *Chem. Rev.* **2014**, *114*, 4175 – 4205.
[2] a) Y. Umena, K. Kawakami, J.-R. Shen, N. Kamiya, *Nature* **2011**, *473*, 55 – 60; b) C. Glöckner, J. Kem, M. Broser, A. Zouni, V. Yachandra, J. Yano, *J. Biol. Chem.* **2013**, *288*, 22607 – 22620; c) N. Cox, D. A. Pantazis, F. Neese, W. Lubitz, *Acc. Chem. Res.* **2013**, *46*, 1588 – 1596; d) P. E. M. Siegbahn, *Biochim. Biophys. Acta Bioenerg.* **2013**, *1827*, 1003 – 1009; e) R. J. Service, W. Hillier, R. J. Debus, *Biochemistry* **2014**, *53*, 1001 – 1017; f) D. Shevela, J. Messinger, *Front. Plant Sci.* **2013**, *4*, 473.
[3] G. C. Dismukes, R. Brimblecombe, G. A. N. Felton, R. S. Pryadun, J. E. Sheats, L. Spiccia, G. F. Swiegers, *Acc. Chem. Res.* **2009**, *42*, 1935 – 1943.
[4] R. Pal, C. F. A. Negre, L. Vogt, R. Pokhrel, M. Z. Ertem, G. W. Brudvig, V. S. Batista, *Biochemistry* **2013**, *52*, 7703 – 7706.
[5] A. Sartorel, M. Bonchio, S. Campagna, F. Scandola, *Chem. Soc. Rev.* **2013**, *42*, 2262 – 2280.
[6] a) R. Al-Oweini, B. S. Bassil, J. Friedl, V. Kottisch, M. Ibrahim, M. Asano, B. Keita, G. Novitchi, Y. Lan, A. Powell, U. Stimming, U. Kortz, *Inorg. Chem.* **2014**, *53*, 5663 – 5673; b) the β-analogue of Mn_4POM, $[Mn^{III}_3Mn^{IV}O_3(CH_3COO)_3(A\text{-}\beta\text{-}SiW_9O_{34})]^{6-}$, which was initially identified only as a co-crystallization product (X. Fang, K. McCallum, H. D. Pratt III, T. M. Anderson, K. Dennis, M. Luban, *Dalton Trans.* **2012**, *41*, 9867 – 9870), has recently been obtained in pure form; see Ref. [6a].
[7] X. K. Fang, M. Speldrich, H. Schilder, R. Cao, K. P. O'Halloran, C. L. Hill, P. Kögerler, *Chem. Commun.* **2010**, *46*, 2760 – 2765.
[8] a) S. Wang, H.-L. Tsai, E. Libby, K. Folting, W. E. Streib, D. N. Hendrickson, G. Christou, *Inorg. Chem.* **1996**, *35*, 7578 – 7589; b) D. N. Hendrickson, G. Christou, E. A. Schmitt, E. Libby, J. S. Bashkin, S. Wang, H. L. Tsai, J. B. Vincent, P. D. W. Boyd, *J. Am. Chem. Soc.* **1992**, *114*, 2455 – 2471; c) Q. Li, J. B. Vincent, E. Libby, H.-R. Chang, J. C. Huffman, P. D. W. Boyd, G. Christou, D. N. Hendrickson, *Angew. Chem. Int. Ed. Engl.* **1988**, *27*, 1731 – 1733; *Angew. Chem.* **1988**, *100*, 1799 – 1801; d) J. S. Kanady, E. Y. Tsui, M. W. Day, T. Agapie, *Science* **2011**, *333*, 733 – 736.
[9] Control CV experiments were run in buffer solution with an unpolished working electrode that was recovered after a Mn_4POM CV scan; a major abatement of the catalytic wave was observed, which indicates that electrodeposition of active Mn-based catalysts is negligible (Figure S1).
[10] UV/Vis spectra of Mn_4POM/$[Ru(bpy)_3]^{2+}$ mixtures confirm that the catalyst is not competing with the sensitizer for light absorption in both laser flash photolysis and photocatalytic experiments (Figure S2).
[11] a) Quenching of $*[Ru(bpy)_3]^{2+}$ by Mn_4POM is negligible as the emission intensity of $[Ru(bpy)_3]^{2+}$ is not affected by Mn_4POM (Figure S3); see: b) M. Natali, M. Orlandi, S. Berardi, S. Campagna, M. Bonchio, A. Sartorel, F. Scandola, *Inorg. Chem.* **2012**, *51*, 7324 – 7331.
[12] The generation of S_n states with $n > 4$ could indeed be envisaged in the catalytic cycle; see: S. Piccinin, A. Sartorel, G. Aquilanti, A. Goldoni, M. Bonchio, S. Fabris, *Proc. Natl. Acad. Sci. USA* **2013**, *110*, 4917 – 4922.
[13] W. J. Youngblood, S. H. A. Lee, Y. Kobayashi, E. A. Hernandez-Pagan, P. G. Hoertz, T. A. Moore, A. L. Moore, D. Gust, T. E. Mallouk, *J. Am. Chem. Soc.* **2009**, *131*, 926 – 927.
[14] a) Photoinduced ET with bimolecular k values of up to $8.7 \times 10^6\,M^{-1}\,s^{-1}$ has been reported for dinuclear Mn^{II} polyazotated complexes; see: P. Huang, A. Magnuson, R. Lomoth, M. Abrahamsson, M. Tamm, L. Sun, B. van Rotterdam, J. Park, L. Hammarstrom, B. Akermark, S. Styring, *J. Inorg. Biochem.* **2002**, *91*, 151; b) under analogous conditions, ET from the Weakley-type tetramanganese POM $[Mn^{II}_4(H_2O)_2(\alpha\text{-}SiW_9O_{34})_2]^{12-}$ (see Ref. [20]) occurs with $k = 3.6 \times 10^9\,M^{-1}\,s^{-1}$. It is noteworthy that the related Wells-Dawson mixed-valent POM $[Mn^{III}_3Mn^{IV}O_3(CH_3COO)_3(\alpha\text{-}P_2W_{15}O_{56})]^{8-}$ (see Ref. [7]) is responsible for a major quenching of the $*[Ru(bpy)_3]^{2+}$ excited state (Figure S4), which hampers a reliable determination of the rate constant for photoinduced ET.
[15] M. Natali, S. Berardi, A. Sartorel, M. Bonchio, S. Campagna, F. Scandola, *Chem. Commun.* **2012**, *48*, 8808 – 8810.
[16] The actual integrity of the aqueous solution state of Mn_4POM was confirmed by conductometric titration experiments with $[Ru(bpy)_3]^{2+}$, resulting in an equivalence point at which three $[Ru(bpy)_3]^{2+}$ ions balance the sixfold negative charge of the polyanion (Figure S5).
[17] For the sake of comparison, both $[Mn^{II}_4(H_2O)_2(\alpha\text{-}SiW_9O_{34})_2]^{12-}$ and $[Mn^{III}_3Mn^{IV}O_3(CH_3COO)_3(\alpha\text{-}P_2W_{15}O_{56})]^{8-}$ show a single ET to $[Ru(bpy)_3]^{3+}$ on the 50 ms time scale (Figure S7, Ref. [14]).
[18] a) M. M. Najafpour, T. Ehrenberg, M. Wiechen, P. Kurz, *Angew. Chem. Int. Ed.* **2010**, *49*, 2233 – 2237; *Angew. Chem.* **2010**, *122*, 2281 – 2285; b) M. M. Najafpour, *Dalton Trans.* **2011**, *40*, 3793 – 3795; c) C. Tommos, G. T. Babcock, *Biochim. Biophys. Acta Bioenergetics* **2000**, *1458*, 199 – 219; d) TOF values of up to $0.35 \times 10^{-3}\,s^{-1}$ were observed for highly defective Ca-doped Mn oxides; see Table S3.
[19] The catalytic activity of Mn_4POM can be also compared to that of a recently reported dimanganese coordination complex with TON ≈ 1; see: E. A. Karlsson, B.-L. Lee, T. Åkermark, E. V. Johnston, M. D. Kärkäs, J. Sun, Ö. Hansson, J.-E. Bäckvall, B. Åkermark, *Angew. Chem. Int. Ed.* **2011**, *50*, 11715 – 11718; *Angew. Chem.* **2011**, *123*, 11919 – 11922.
[20] U. Kortz, S. Isber, M. H. Dickman, D. Ravot, *Inorg. Chem.* **2000**, *39*, 2915.

